The Journal of Immunology

Anti-Inflammatory Activity of PYNOD and Its Mechanism in Humans and Mice

Ryu Imamura, Yetao Wang, Takeshi Kinoshita, Misao Suzuki, Tetsuo Noda, Junji Sagara, Shun'ichiro Taniguchi, Hiroshi Okamoto and Takashi Suda

J. Immunol. 2010;184;5874-5884; originally published online Apr 14, 2010;
doi:10.4049/jimmunol.0900779
http://www.jimmunol.org/cgi/content/full/184/10/5874

The Journal of Immunology is published twice each month by The American Association of Immunologists, Inc., 9650 Rockville Pike, Bethesda, MD 20814-3994.

Print ISSN: 0022-1767 Online ISSN: 1550-6606.

Anti-Inflammatory Activity of PYNOD and Its Mechanism in Humans and Mice

Ryu Imamura,* Yetao Wang,* Takeshi Kinoshita,* Misao Suzuki,† Tetsuo Noda,‡ Junji Sagara,§ Shun'ichiro Taniguchi,§ Hiroshi Okamoto,¶ and Takashi Suda*

Many members of the nucleotide-binding and oligomerization domain (NOD)- and leucine-rich-repeat–containing protein (NLR) family play important roles in pathogen recognition and inflammation. However, we previously reported that human PYNOD/NLRP10, an NLR-like protein consisting of a pyrin domain and a NOD, inhibits inflammatory signal mediated by caspase-1 and apoptosis-associated speck-like protein containing a caspase recruitment domain (ASC) in reconstitution experiments using HEK293 cells. In this study, we investigated the molecular mechanism of PYNOD's anti-inflammatory activity in vitro and its expression and function in mice. Human PYNOD inhibited the autoprocessing of caspase-1 and caspase-1–mediated IL-1β processing and suppressed the aggregation of ASC, a hallmark of ASC activation. Interestingly, the NOD of human PYNOD was sufficient to inhibit caspase-1–mediated IL-1β secretion, whereas its pyrin domain was sufficient to inhibit ASC-mediated NF-κB activation and apoptosis and to reduce ASC's ability to promote caspase-1–mediated IL-1β production. Mouse PYNOD protein was detected in the skin, tongue, heart, colon, peritoneal macrophages, and several cell lines of hematopoietic and myocytic lineages. Mouse PYNOD colocalized with ASC aggregates in LPS + R837-stimulated macrophages; however, unlike human PYNOD, mouse PYNOD failed to inhibit ASC aggregation. Macrophages and neutrophils from PYNOD-transgenic mice exhibited reduced IL-1β processing and secretion upon microbial infection, although mouse PYNOD failed to inhibit caspase-1 processing, which was inhibited by caspase-4 inhibitor z-LEED-fluoromethylketone. These results suggest that mouse PYNOD colocalizes with ASC and inhibits caspase-1–mediated IL-1β processing without inhibiting caspase-4 (mouse caspase-11)–mediated caspase-1 processing. Furthermore, PYNOD-transgenic mice were resistant to lethal endotoxic shock. Thus, PYNOD is the first example of an NLR that possesses an anti-inflammatory function in vivo. ***The Journal of Immunology*****, 2010, 184: 5874–5884.**

A large family of animal proteins containing the nucleotide-binding and oligomerization domain (NOD) and leucine-rich repeats (LRRs), and thus called NLRs, has recently emerged (1, 2). These proteins typically have an additional protein interaction domain, such as a pyrin domain (PYD) or a caspase recruitment domain (CARD). Many of them play important roles as pathogen or danger-signal sensors that activate inflammatory responses. For example, Nod1 (also called NLRC1, CARD4, and CLR7.1) and Nod 2 (also called NLRC2, CARD15, and CLR16.3) recognize distinct portions of different types of peptidoglycans and activate NF-κB (3). Other NLRs, such as NLRP1 (also called NALP1, DEFCAP, CARD7, CLR17.1, and NAC), NLRP3 (also called PYPAF1, cryopyrin, NALP3, and CLR1.1), and NLRC4 (also called CARD12, Ipaf, CLAN, and CLR2.1) form an inflammasome, the molecular platform for caspase-1 activation, which leads to the proteolytic maturation of inflammatory cytokines, such as IL-1β and IL-18, in response to various pathogen-related molecules (such as flagellin, bacterial and viral RNA, LPS, and muramyl dipeptide) and inorganic inflammatory substances (such as uric acid crystals and asbestos) (4, 5). The latter group of NLRs interacts with apoptosis-associated speck-like protein containing a CARD (ASC), an adaptor protein consisting of a PYD and a CARD. ASC links these NLRs with caspase-1, caspase-8, or both and plays an essential role in caspase-1 activation (6–8), caspase-8–mediated apoptosis, or both and NF-κB activation (9, 10).

In contrast, we previously discovered a novel NLR-like protein that shows anti-inflammatory activity in vitro. It consists of a PYD and a NOD; however, unlike other NLRs, it lacks LRRs. Therefore, we named it PYNOD (also called NLRP10, NALP10, CLR11.1, Nod8, and PAN5) (11). Reconstitution experiments using HEK293 cells revealed that human PYNOD can inhibit caspase-1–dependent IL-1β secretion and ASC-mediated NF-κB activation and apoptosis. This was one of the first examples of an NLR family member that plays a negative regulatory role in IL-1β secretion. Others and we have also reported that human NLRP2 (also called PYPAF2, NALP2, CLR19.9, NBS1, and PAN1), NLRP7 (also called PYPAF3, NALP7, CLR19.4, Nod12, and PAN7), NLRP4 (also called PYPAF4, NALP4, CLR19.5, PAN2, and RNH2), NLRP12 (also called PYPAF7, NALP12, FCAS2, PAN6, CLR19.3,

*Division of Immunology and Molecular Biology, Cancer Research Institute, Kanazawa University, Kanazawa; †Division of Transgenic Technology, Center for Animal Resources and Development, Institute of Resource Development and Analysis, Kumamoto University, Kumamoto; ‡Department of Cell Biology, Cancer Institute, Japanese Foundation of Cancer Research, Tokyo; §Department of Molecular Oncology, Institute on Aging and Adaptation, Shinshu University Graduate School of Medicine, Matsumoto; and ¶Department of Advanced Biological Sciences for Regeneration, Tohoku University Graduate School of Medicine, Sendai, Japan

Received for publication March 10, 2009. Accepted for publication March 16, 2010.

This work was supported in part by Grants-in-Aid for Scientific Research on Priority Areas (Cancer) from the Ministry of Education, Culture, Sports, Science and Technology of Japan.

Address correspondence and reprint requests to Dr. Takashi Suda, Division of Immunology and Molecular Biology, Cancer Research Institute, Kanazawa University, Kakumamachi, Kanazawa, Ishikawa 920-1192, Japan. E-mail address: sudat@kenroku.kanazawa-u.ac.jp

The online version of this article contains supplemental material.

Abbreviations used in this paper: ASC, apoptosis-associated speck-like protein containing a caspase recruitment domain; CARD, caspase recruitment domain; cmk, chloromethylketone; fmk, fluoromethylketone; HA, human influenza virus hemagglutinin epitope; LRR, leucine-rich repeat; moi, multiplicity of infection; NLR, nucleotide-binding and oligomerization domain- and LRR-containing protein; NOD, nucleotide-binding and oligomerization domain; PEC, peritoneal exudate cell; PI, propidium iodide; PYD, pyrin domain; RLA, relative luciferase activity.

www.jimmunol.org/cgi/doi/10.4049/jimmunol.0900779

and Monarch-1), NLRC3 (also called CLR16.2 and Nod3), NLRX1 (also called CLR11.3 and Nod9), and Nod2-S, a short splicing variant of Nod2, have anti-inflammatory or immunosuppressive functions (12–17). Thus, it is likely that the NLR family includes an anti-inflammatory subgroup. However, the in vivo functions of these anti-inflammatory NLRs have not been explored.

In this study, we first examined the molecular mechanisms of the anti-inflammatory function of human PYNOD. In addition, to examine the in vivo functions of PYNOD, we generated PYNOD-transgenic mice and investigated the production of cytokines by their inflammatory cells and the animals' resistance to lethal endotoxic shock. The results presented in this paper provide further evidence that PYNOD acts as a negative regulator of inflammation in vivo.

Materials and Methods

Plasmids

Expression plasmids carrying human cDNAs for PYNOD with or without a Myc or FLAG tag, NLRP2, NLRP3, LRR-truncated NLRC4 (aa 1–457), ASC, FLAG-tagged caspase-1, IL-1β with or without a human influenza virus hemagglutinin epitope (HA) tag, Fas, and truncated Bid (aa 61–195) and the expression plasmid for mouse PYNOD were described previously (11, 12, 18). Expression plasmids carrying cDNAs encoding Myc- or FLAG-tagged PYD (aa 1–87) or NOD (aa 82–655) from human PYNOD and expression plasmids for mouse IL-1β and caspase-1 with or without FLAG tag were generated in this study (Supplemental Table 1). To generate pCAGGS-LGL-mPYNOD, the GFP gene with a poly-A signal sequence and mouse PYNOD cDNA from pEF-mPYNOD were cloned into a loxP plasmid pULwL (19) (provided by Dr. Masahide Asano, Advanced Science Research Center, Kanazawa University, Ishikawa, Japan). A DNA fragment containing the loxP-GFP-loxP-mPYNOD construct was then cloned into the mammalian pCAGGS expression vector (20). The pCAGGS-Cre plasmid (21) was kindly provided by Dr. Nobuyuki Takakura (Research Institute for Microbial Diseases, Osaka University).

Establishment of anti-human ASC and anti-mouse PYNOD mAbs

To generate an anti-human ASC mAb, BALB/c mice were immunized with a human ASC fragment (aa 113–195). To generate an anti-mouse PYNOD and anti-mouse ASC mAb, Wistar rats were immunized with a mouse PYNOD fragment (aa 516–638) and full-length mouse ASC, respectively. Lymph node cells from the immunized animals were fused with the P3U1 mouse myeloma cell line, and hybridoma clones producing an Ab specific to the corresponding Ag were established as described previously (22). The mouse and rat mAbs were purified using protein A and protein G Sepharose Fast Flow columns (GE Healthcare, Amersham, U.K.), respectively.

Cells and culture conditions

The HEK293, HEK293T, and HEK293T-Y human embryonic kidney cell lines (11) and the C_2C_{12}, C7 (23), J774A.1, N1E-115, and RAW264.7 mouse cell lines were cultured in 10% FCS-DMEM. The A3.4C6, A20.2J, BAF/BO3, DC2.4 (24), and EL4 mouse cell lines were cultured in 10% FCS-RPMI 1640. The DC2.4 cell line was established by Dr. Kenneth L. Rock (University of Massachusetts Medical School, Worcester, MA) and provided by the Dana-Farber Cancer Institute (Boston, MA).

Thioglycollate-induced 4-h and 4-d peritoneal exudate cells (PECs) were prepared as described previously (25). The 4-d PECs (1×10^5 cells/well) were cultured in a 96-well plate for 2 h, and the nonadherent cells were then removed. To induce cytokine production, adherent macrophages were cultured in RPMI 1640 medium supplemented with 10% FCS, penicillin, and streptomycin, with or without LPS (1 μg/ml, from *Escherichia coli* 055:B5; Sigma-Aldrich, St. Louis, MO) overnight. In some experiments, LPS-primed macrophages were pretreated with inhibitors, such as z-LEED–fluoromethylketone (fmk) (MBL, Nagoya, Japan), z-VAD–fmk, and Ac-YVAD–chloromethylketone (cmk) (Calbiochem, La Jolla, CA), or DMSO as the solvent control for 1 h. The cells were washed with fresh culture medium that lacked antibiotics and then infected with *Salmonella typhimurium* (ATCC 14028s) at a multiplicity of infection (moi) of 10, 20, or 50 or stimulated with R837 (10 μg/ml; InvivoGen, San Diego, CA) for 12 h. After 1 h of *S. typhimurium* infection, gentamycin (final concentration of 50 μg/ml) was added to kill the extracellular bacteria. Whole 4-h PECs (1×10^5 cells/well) were cultured in a 96-well plate, stimulated, infected, or both as described above, except that the cells were cultured in antibiotic-free medium from the beginning and were not washed after the LPS pretreatment.

Mice

The floxed GFP–PYNOD-tg and PYNOD-tg mice were established as described in the *Results*. Transgene-positive mice were identified by PCR using the following primers: sense, 5′-CTGCTAACCATGTTCATGCC-3′; antisense, 5′-CCCGGTAGATTTCTCTGTAATCAT-3′. Insulin-Cre-tg mice expressing Cre under control of the insulin promoter (26) and $ASC^{-/-}$ mice (27) were described previously. C57BL/6 mice were purchased from Japan SLC (Shizuoka, Japan). Lethal endotoxic shock was induced by the i.p. administration of LPS (from *E. coli* 0111:B4, Sigma-Aldrich). All of the animal protocols used in this study were approved by the Kanazawa University Committee on Animal Welfare.

Transient transfection

HEK293, HEK293T, and HEK293T-Y cells were transfected with plasmid DNAs using Lipofectamine PLUS reagents (Invitrogen, Carlsbad, CA), according to the manufacturer's protocol or, for reporter assays, linear polyethylenimine (M_r ~25,000; Polysciences, Warrington, PA), as described previously (9). The total amount of transfected DNA was kept constant within each experiment using empty vector.

Immunoprecipitation and Western blot analysis

Immunoprecipitation and Western blots were carried out as previously described (11). Mouse PYNOD and IL-1β were immunoprecipitated using an anti-mouse PYNOD mAb (established in this study) and hamster anti-mouse IL-1β mAb (Santa Cruz Biotechnology, Santa Cruz, CA), respectively. The following Abs were used for Western blots: anti-FLAG (M2) and anti-HA (HA7) mAbs (Sigma-Aldrich), anti-mouse PYNOD and human ASC mAbs (established in this study), anti-Myc, anti-GAPDH, and anti-GFP mAbs (MBL), polyclonal goat anti-mouse IL-1β Ab (Techne Corp., Minneapolis, MN), and polyclonal rabbit anti-mouse caspase-1 Ab (Santa Cruz Biotechnology).

Measurement of cytokines

The amount of mouse IL-1β, TNF-α, and IL-6 in culture supernatants was determined using OptEIA ELISA kits (BD Pharmingen, San Diego, CA), according to the manufacturer's protocols.

NF-κB reporter assay

The NF-κB reporter assay was performed as described previously (9). In brief, HEK293 cells were transfected with 50 ng pNF-κB-Luc (Stratagene, Cedar Creek, TX) and 10 ng pRL-TK (Promega, Madison, WI) together with other plasmids. The firefly and renilla luciferase activity was measured 24 h after transfection using the Dual-Luciferase Reporter Assay System (Promega). The fold induction of NF-κB activity = experimental relative luciferase activity (RLA)/RLA of vector control, where RLA = firefly luciferase activity/renilla luciferase activity.

Apoptosis assay

The induction of apoptosis by exogenous gene expression was evaluated as described previously (11). In brief, apoptosis-sensitive HEK293T-Y cells were transfected with test genes together with pEGFP-C1 (BD Clontech, Mountain View, CA). Twenty-four hours later, the cells were stained with propidium iodide (PI) and Cy5-annexin V (BioVision, Palo Alto, CA) and analyzed by flow cytometry. The proportion of apoptotic cells was determined as the percentage of GFP^+ cells that were $Cy5^+PI^-$.

Immunofluorescence confocal microscopy

Immunofluorescence confocal microscopy was carried out as previously described (9). Myc-tagged PYNOD was detected using a FITC-conjugated goat anti–c-Myc Ab (Bethyl, Montgomery, TX). Human ASC was detected using the mouse mAb established in this study followed by Alexa Fluor 594-goat anti-mouse IgG1 (Molecular Probes, Eugene, OR). Mouse ASC was detected using a polyclonal rabbit Ab (provided by Dr. Junji Sagara, School of Health Sciences, Shinshu University, Matsumoto, Japan) or rat mAb established in this study followed by FITC-conjugated anti-rabbit IgG (Jackson ImmunoResearch Laboratories, West Grove, PA) or Cy3-conjugated goat anti-rat IgG (Chemicon, Temecula, CA). Mouse PYNOD was detected using the rat mAb established in this study followed by Cy3-conjugated goat anti-rat IgG. In some experiments, nuclei were stained with DAPI (Dojindo, Kumamoto, Japan). For fluorescein labeling, macrophages (10^7 cells/ml) were incubated with 20 μM CFSE (Dojindo) in RPMI 1640 medium for 15 min at 37°C. CFSE staining was stopped by adding excess RPMI 1640 medium and washing cells twice with RPMI 1640 medium.

Statistical analysis

The statistical significance of data was evaluated by a two-tailed Student *t* test. A p value <0.05 was considered significant.

Results

Human PYNOD inhibits the processing of procaspase-1 and pro–IL-1β via its NOD

We previously reported that human PYNOD inhibits caspase-1–mediated IL-1β release by reconstitution experiments using HEK293 cells (11). To explore the precise molecular mechanism of this inhibition, we investigated whether PYNOD inhibits the processing of procaspase-1 and caspase-1–dependent pro–IL-1β maturation. For this purpose, NLRP2 or PYNOD was coexpressed with pro–IL-1β and procaspase-1 or with procaspase-1 in HEK293T cells, and the expression of the mature form of IL-1β (p17) or the N-terminal fragment of procaspase-1 (p35) was assessed by Western blot (Fig. 1*A*, 1*B*). When mutant procaspase-1 (mutation in catalytic site) was used in this experiment, the p35 fragment was not detected, suggesting that caspase-1 was processed by an autocatalytic mechanism in this system (data not shown). NLRP2 was used as a control for PYNOD, because we previously found that NLRP2 inhibits ASC-mediated NF-κB activation but not caspase-1–mediated IL-1β processing (12). Under these conditions, PYNOD but not human NLRP2 dose-dependently inhibited the generation of p17 and p35. These results indicate that PYNOD inhibits the procaspase-1 processing. The inhibition of p17 production may have resulted from the direct inhibition of IL-1β cleavage or as an indirect result from the proteolytic activation of caspase-1.

To determine the region of PYNOD that is essential for its inhibitory activity against caspase-1, the PYD or NOD of PYNOD or full-length PYNOD was coexpressed with procaspase-1 and pro–IL-1β in HEK293 cells, and the amount of IL-1β secreted into the culture supernatant was determined by ELISA (Fig. 1*C*). The results indicated that the NOD alone as well as full-length PYNOD inhibited IL-1β secretion, whereas the PYD showed no inhibitory activity in this assay system. Consistently, when caspase-1 was immunoprecipitated from the lysate of HEK293T cells transfected with caspase-1 and the full-length, NOD, or PYD of PYNOD, the full-length and NOD of PYNOD were coprecipitated, whereas its PYD was not (Fig. 1*D*). Thus, the NOD of PYNOD is essential and sufficient to interact with caspase-1 and to inhibit caspase-1–mediated IL-1β maturation.

Human PYNOD inhibits ASC-mediated IL-1β secretion, NF-κB activation, and apoptosis via its PYD

PYNOD also inhibits the functions of ASC. One of ASC's functions is to promote caspase-1 activity, especially in the presence of NLRP3. Therefore, we further investigated which region of PYNOD is required to inhibit the IL-1β secretion induced by the coexpression of NLRP3, ASC, procaspase-1, and pro–IL-1β (Fig. 1*E*). In this system, not only the NOD and full-length PYNOD but also the PYD of PYNOD inhibited the IL-1β secretion. Because the PYD of PYNOD did not inhibit IL-1β production induced by caspase-1 overexpression, it is likely that the PYD inhibited the ASC's function to enhance caspase-1–mediated IL-1β secretion. We previously demonstrated that human ASC also induces NF-κB activation and apoptosis in HEK293 cells and that these functions of ASC are augmented by the coexpression of a constitutively active, LRR-truncated form of NLRC4 (NLRC4ΔLRR) (9, 10). PYNOD inhibits the ASC-mediated NF-κB activation and apoptosis but does not inhibit Bid-induced apoptosis (11). Interestingly, the PYD and full-length PYNOD, but not the NOD of PYNOD, strongly inhibited the NF-κB activation induced by the coexpression of ASC and NLRC4ΔLRR (Fig. 2*A*) as well as the apoptosis induced by a high dose of ASC alone or by ASC and NLRC4ΔLRR; in contrast, none of the constructs significantly inhibited Bid-induced apoptosis (Fig. 2*B*). These results indicate that the PYD is essential and sufficient for human PYNOD's inhibition of ASC.

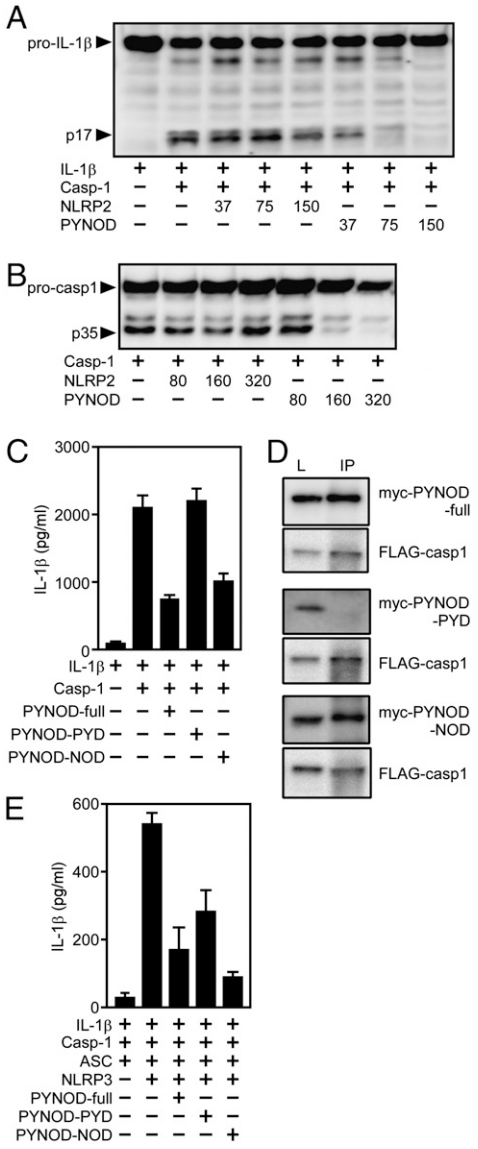

FIGURE 1. Human PYNOD inhibits the processing of procaspase-1 and pro–IL-1β via NOD. *A* and *B*, HEK293T cells (2×10^5) were transfected with expression plasmids carrying human cDNAs for C-terminal HA-tagged pro–IL-1β (200 ng) and procaspase-1 (50 ng) (*A*) or for N-terminal FLAG-tagged procaspase-1 (160 ng) (*B*) with or without the indicated amounts (in nanograms) of expression plasmid for human NLRP2 or PYNOD. After 24 h of culture, cell lysates were prepared and analyzed by Western blot using an anti-HA (*A*) or anti-FLAG Ab (*B*). *C* and *E*, HEK293 cells (4×10^4) were transfected with expression plasmids carrying human cDNAs for pro–IL-1β (150 ng), procaspase-1 (25 ng), or both (*C*) or for pro–IL-1β (120 ng), procaspase-1 (2.5 ng), ASC (5 ng), and NLRP3 (25 ng) (*E*) with or without an expression plasmid (150 ng) for the full-length, PYD, or NOD of human PYNOD. Supernatants were analyzed for IL-1β secretion by ELISA 24 h after transfection. Experiments were done in duplicate, and error bars represent the range of duplicate samples. Data are representative of at least three independent experiments. *D*, HEK293T cells (1×10^5) were transfected with an expression plasmid carrying a human cDNA for FLAG-tagged procaspase-1 (500 ng) together with an expression plasmid for the Myc-tagged full-length, PYD, or NOD of human PYNOD (500 ng) as indicated. After 24 h of culture, cell lysates were prepared, and the immunoprecipitates using anti-FLAG Ab were examined by Western blot using an anti-Myc or anti-FLAG Ab. The expression of FLAG- and Myc-tagged proteins in total cell lysates was also examined by Western blot.

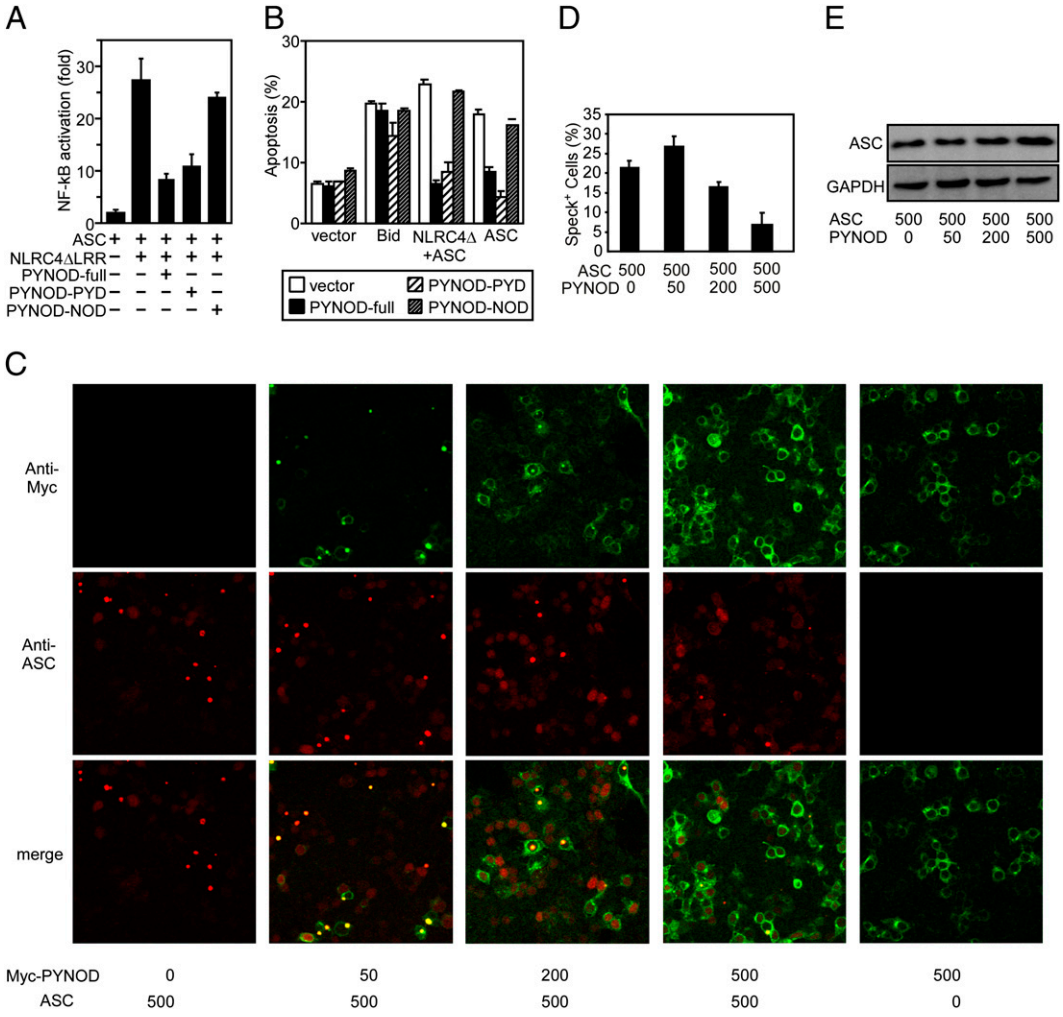

FIGURE 2. Human PYNOD inhibits ASC's functions via its PYD and prevents ASC aggregation. *A*, HEK293 cells (4×10^4) were transfected with expression plasmids carrying human cDNAs for ASC (25 ng), NLRC4ΔLRR (100 ng), and/or the full-length, PYD, or NOD of human PYNOD (150 ng) together with an NF-κB reporter plasmid. NF-κB activity was determined by luciferase reporter assay. *B*, HEK293T-Y cells (3×10^4) were transfected with expression plasmids carrying human cDNAs for active Bid (60 ng), ASC (60 ng), or NLRC4ΔLRR (20 ng) plus ASC (4 ng) with or without an expression plasmid for the full-length, PYD, or NOD of human PYNOD (60 ng). The proportion of apoptotic cells (Cy5-annexin V-positive and PI-negative cells) was determined 24 h after transfection using flow cytometry. Experiments were done in duplicate, and error bars represent the range of duplicate samples. Data are representative of at least three independent experiments. *C*, HEK293T cells (5×10^5) were transfected with the indicated amounts (in nanograms) of expression plasmids for human ASC, Myc-tagged human PYNOD, or both and cultured on glass coverslips. After cell fixation, the proteins were detected using anti-ASC polyclonal Ab followed by Alexa Fluor 594-goat anti-mouse IgG1 (red) and FITC-conjugated anti-Myc mAb (green). Merged images are also shown (merge). Original magnification ×100. *D*, Experiments were performed as described in *C*, and total cells and cells with an ASC aggregate (speck) were counted in 10 microscopic fields per group. Experiments were done twice, and the mean percentage of speck-positive cells and its range in the two experiments are shown. *E*, Expression levels of ASC in the transfected cells in *C* were examined by Western blot using anti-ASC mAb. Western blot for GAPDH serves as a loading control.

Human PYNOD inhibits ASC aggregation

Activated ASC forms large aggregates in cells (28). We previously found that PYNOD was coprecipitated with ASC from lysates of HEK293 cells expressing both proteins (11). Therefore, we investigated the effect of PYNOD on ASC aggregation. As shown in Fig. 2*C* and Supplemental Fig. 1, ASC overexpressed in a HEK293T cell formed a single large aggregate called a speck, although cells with multiple ASC aggregates were occasionally observed. In contrast, PYNOD expressed without ASC distributed in the cytosol. When a small amount of PYNOD was coexpressed with ASC under similar conditions, the PYNOD was colocalized with the ASC aggregates. However, when the amount of PYNOD was increased, it gradually exhibited a diffuse distribution in the cytosol and inhibited the aggregation of ASC. Increasing the amount of the PYNOD expression vector reduced the proportion of ASC aggregate-positive cells (Fig. 2*D*). Western blot analysis indicated that the expression level of ASC was not changed by the coexpression of PYNOD (Fig. 2*E*). These results indicate that human PYNOD can inhibit the aggregation of ASC.

Expression profile of mouse PYNOD protein in tissues and cells

To explore the function of PYNOD in vivo, we first investigated its expression profile in mouse using a newly raised mAb against mouse PYNOD. This mAb specifically recognized a 70-kDa protein in cell extracts from mouse PYNOD-transfected but not mock-transfected HEK293T cells and did not cross-react with mouse NLRP2, NLRP3, NLRC4, ASC, and caspase-1 and human PYNOD and NLRP3 (Supplemental Fig. 2*A*). A corresponding 70-kDa protein was detected by immunoprecipitation followed by Western blot (Fig. 3*A*) in several mouse cell lines: BAF/BO3 (pre-B), C7 (macrophage), RAW264.7 (macrophage), DC2.4 (dendritic), and C_2C_{12} (myoblast). However, it was not detected in A20.2J (B), A3.4C6 (T), EL4

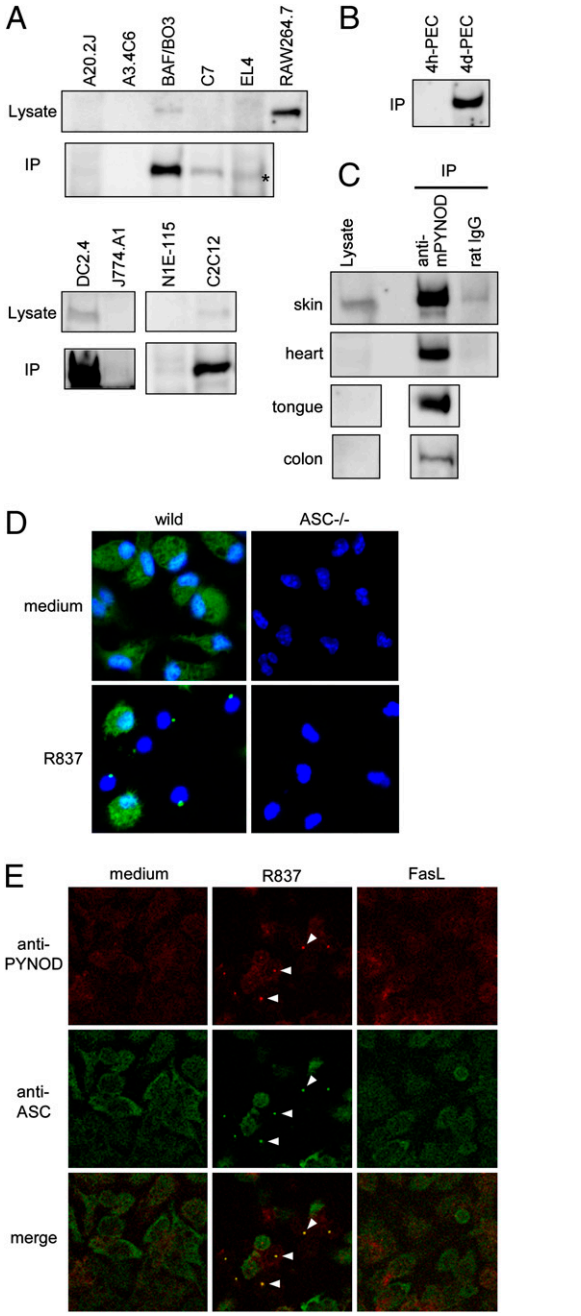

FIGURE 3. Expression profile of mouse PYNOD and colocalization of PYNOD with ASC in activated macrophages. *A–C*, Mouse PYNOD protein in whole extracts (lysate) of cells or tissues or immunoprecipitates from the lysates using rat anti-mouse PYNOD mAb (*A–C*) or normal rat IgG (*C*) was visualized by Western blot. The asterisk in *A* indicates a nonreproducible band slightly smaller than PYNOD. *D*, Thioglycollate-induced peritoneal macrophages from wild-type and $ASC^{-/-}$ mice were cultured on glass coverslips and pretreated with LPS for 16 h. The LPS-primed macrophages were then stimulated by R837 (50 μg/ml) for 2 h. The cells were fixed, and proteins were detected using an anti-mouse ASC polyclonal Ab followed by FITC-conjugated anti-rabbit IgG (green). The nuclei were counterstained with DAPI (blue). Original magnification ×200. *E*, LPS-primed macrophages were stimulated by R837 as in *D* or by Fas ligand (4000 U/ml). The cells were fixed, and proteins were detected using an anti-mouse ASC polyclonal Ab followed by FITC-conjugated anti-rabbit IgG (green) and anti-PYNOD mAb followed by Cy3-conjugated anti-rat IgG (red). Merged images are also shown (merge). Arrowheads indicate ASC aggregates and colocalization with PYNOD. Original magnification ×170.

(T), J774.A1 (macrophage), or N1E-115 (neuroblast) cells. The PYNOD protein was also detected in macrophages isolated from 4-d PECs but not in neutrophil-rich 4 h PECs (Fig. 3*B*). PYNOD expressed in 4-d PECs was specifically detected by Western blot using this mAb (Supplemental Fig. 2*B*). Among the tissues that we examined, PYNOD was detected in the skin, tongue, heart, and colon but not in the kidney, skeletal muscle, spleen, liver, lung, thymus, brain, or small intestine (Fig. 3*C* and data not shown).

PYNOD colocalizes with ASC in peritoneal macrophages after R837 stimulation

Because human PYNOD colocalized with ASC in HEK293T cells, we next examined whether endogenous PYNOD and ASC colocalized in macrophages isolated from 4-d PECs. Immunostaining using anti-mouse ASC polyclonal Ab detected a single large perinuclear aggregate of ASC in a macrophage stimulated with LPS + R837 (Fig. 3*D*), which induces NLRP3- and ASC-dependent caspase-1–mediated IL-1β processing (29). Immunostaining of 4-d PECs from wild-type and $ASC^{-/-}$ mice confirmed the specificity of ASC staining with this Ab. Importantly, endogenous PYNOD colocalized with ASC under these conditions (Fig. 3*E*). In contrast, Fas ligand, which induces caspase-1–independent IL-1β secretion in LPS-primed macrophages (25; Supplemental Fig. 3), did not induce the aggregation of ASC.

Inhibitory effect of mouse PYNOD on caspase-1–mediated IL-1β secretion

To examine the functions of mouse PYNOD, we sought to generate PYNOD-transgenic mice. Because an initial attempt to generate mice that constitutively expressed PYNOD was unsuccessful for unknown reasons, we created a plasmid for the inducible expression of mouse PYNOD (pCAGGS-LGL-mPYNOD) in which the CAG promoter and the cDNA encoding PYNOD were separated by the GFP gene carrying a poly-A signal and flanked by loxP sites (Fig. 4*A*). When HEK293T cells were transfected with this plasmid, the expression of GFP but not PYNOD was detected by Western blot, whereas the reciprocal expression pattern was observed when the cells were cotransfected with pCAGGS-LGL-mPYNOD and a plasmid constitutively expressing Cre recombinase (Fig. 4*B*).

Before making transgenic mice, we tested the effects of mouse PYNOD in vitro. The inhibitory activity of mouse PYNOD against caspase-1–mediated IL-1β secretion was assessed by reconstitution experiments in which IL-1β secretion was induced by the transient cotransfection of procaspase-1 and pro–IL-1β in HEK293 cells. Like human PYNOD (11), the enforced expression of mouse PYNOD under the elongation factor-1α promoter potently inhibited the secretion of IL-1β in this system (Fig. 4*C*). Furthermore, consistent with the expression pattern of mouse PYNOD, the transfection of cells with pCAGGS-LGL-mPYNOD and pCAG-Cre in combination, but not with pCAGGS-LGL-mPYNOD alone, inhibited the IL-1β secretion. These results indicate that mouse PYNOD is capable of inhibiting caspase-1–mediated IL-1β secretion.

Generation of transgenic mice systemically expressing mouse PYNOD

We established inducible PYNOD transgenic (floxed GFP-PYNOD-tg) mice by introducing the PYNOD-expressing construct from the pCAGGS-LGL-mPYNOD plasmid into C57BL/6J mouse zygotes (Fig. 4*D*, *lane 1*). F1 mice were generated by mating the floxed mice with transgenic mice (CD-1 background) expressing Cre under the control of the insulin promoter (26). Mosaic deletion of the GFP gene was found in some F1 mice (Fig. 4*D*, *lanes 2* and *3*). The mosaic F1 mice were further mated with wild-type C57BL/6J mice, and F2 (PYNOD-tg) mice exhibiting uniform GFP gene deletion

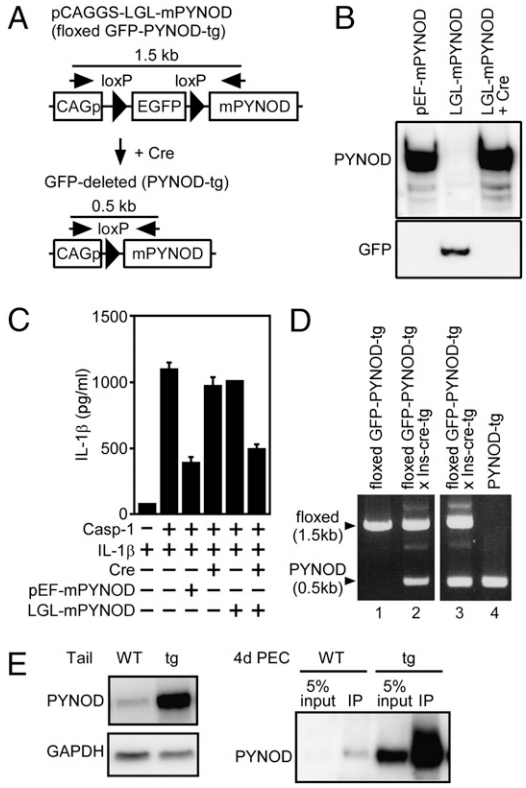

FIGURE 4. Establishment of an inducible expression system for mouse PYNOD and generation of PYNOD-tg mice. *A*, Schematic of the inducible expression unit for mouse PYNOD in the pCAGGS-LGL-mPYNOD expression plasmid and its GFP-deleted form after Cre-mediated recombination. Primer positions for mouse genotyping are indicated by arrows. *B*, HEK293T cells (2×10^5) were transfected with 200 ng of a constitutive (pEF-mPYNOD) or inducible (pCAGGS-LGL-mPYNOD) expression plasmid for mouse PYNOD with or without 200 ng pCAGGS-Cre. Cell lysates were analyzed by Western blot using an anti-PYNOD or anti-GFP mAb. *C*, HEK293 cells (3×10^4) were transfected with expression plasmids for mouse procaspase-1 (50 ng), mouse pro–IL-1β (50 ng), and/or Cre (10 ng) with or without pEF-mPYNOD (20 ng) or pCAGG-LGL-mPYNOD (20 ng). The supernatants were analyzed by ELISA for IL-1β 24 h after transfection. Experiments were done in duplicate, and error bars represent the range of duplicate samples. Data are representative of at least three independent experiments. *D*, PCRs for the genotyping of floxed and PYNOD-tg mice using the primer set shown in *A*. A 1.5-kb DNA fragment corresponded to the floxed allele, whereas a 0.5-kb DNA fragment corresponded to the GFP-deleted allele. *E*, Expression of PYNOD in the lysates of tails and thioglycollate-induced peritoneal macrophages (4-d PECs) from a PYNOD-tg mouse and wild-type littermate was examined by Western blot or immunoprecipitation followed by Western blot. Western blot for GAPDH serves as a loading control.

were isolated (Fig. 4*D*, *lane 4*). High PYNOD protein expression in the PYNOD-tg mice was confirmed by examining extracts from the tail and peritoneal macrophages by immunoprecipitation, Western blot, or both (Fig. 4*E*). The PYNOD-tg mice were viable and fertile and could not be identified from littermates by macroscopic observation. PYNOD-tg mice and wild-type (nontransgenic) littermates with nonuniform mixture of C57BL/6J and CD-1 background were used in the following study.

Peritoneal macrophages from PYNOD-tg mice are defective in the IL-1β production induced by S. typhimurium *infection or R837 stimulation*

Infection with *S. typhimurium* and stimulation with R837 induce caspase-1–mediated IL-1β secretion in macrophages in a NLRC4- and NLRP3-dependent manner, respectively (29, 30). Because ASC also plays an important role in these responses, the macrophages from $ASC^{-/-}$ mice are defective in these responses. To explore the function of PYNOD in macrophages, we compared the release of IL-1β in response to *S. typhimurium* infection or R837 stimulation in LPS-primed peritoneal macrophages from PYNOD-tg mice, their wild-type littermates, and $ASC^{-/-}$ mice (Fig. 5*A*). Like the $ASC^{-/-}$ macrophages, the PYNOD-tg macrophages tended to secrete lower levels of IL-1β than the wild-type macrophages. We further confirmed that the mature form of IL-1β (p17) was reduced in the culture supernatant of the PYNOD-tg and $ASC^{-/-}$ macrophages compared with that in wild-type macrophages after *S. typhimurium* infection (Fig. 5*B*). Unlike the caspase-1–mediated maturation of IL-1β or IL-18, the NF-κB–dependent production of TNF-α and IL-6 are unaffected in $ASC^{-/-}$ macrophages (4, 29, 30). Likewise, the production of TNF-α and IL-6 by the PYNOD-tg macrophages in response to *S. typhimurium* infection was comparable to that of wild-type and $ASC^{-/-}$ macrophages (Fig. 5*C*). These results exclude the possibility that PYNOD-tg macrophages are generally poorly responsive because of a developmental defect or for other reasons.

Neutrophil-rich PECs from PYNOD-tg mice are defective in the IL-1β production induced by S. typhimurium *infection or R837 stimulation*

Because the endogenous expression level of mouse PYNOD was very low in the neutrophil-rich 4-h PECs compared with that in peritoneal macrophages from 4-d PECs (Figs. 3*B*, 5*D*), we also examined the IL-1β release from LPS-primed 4 h PECs in response to *S. typhimurium* infection or R837 stimulation. Flow cytometry analyses indicated that 4 h PECs contained ~85% Gr-1–positive neutrophils and 6% F4/80-positive macrophages (Supplemental Fig. 4). Therefore, the majority of IL-1β produced from total 4-h PECs was estimated to be derived from neutrophils, although macrophage-enriched population derived from 4-h PECs exhibited higher IL-1β production (355 ± 20 pg/ml) per cell than the neutrophil-enriched population (91 ± 20 pg/ml) in response to *S. typhimurium* infection. As in the peritoneal macrophages, a high level of PYNOD protein expression was detected in the 4 h PECs of the PYNOD-tg mice (Fig. 5*D*). In addition, the 4 h PECs from PYNOD-tg and $ASC^{-/-}$ mice secreted lower levels of IL-1β in response to *S. typhimurium* infection or R837 stimulation compared with those from wild-type mice (Fig. 5*E*).

We established another PYNOD-tg mouse line (PYNOD-tg2) independent of the PYNOD-tg line described above. Dot blot analyses indicated that the copy numbers of the transgene in PYNOD-tg and PYNOD-tg2 were 3 and 2, respectively (data not shown). PYNOD-tg2 mice exhibited lower levels of PYNOD overexpression compared with those in the PYNOD-tg mice (Fig. 5*D*). The 4 h PECs from PYNOD-tg2 mice secreted lower levels of IL-1β than those from wild-type mice (Fig. 5*F*), although the peritoneal macrophages from 4-d PECs of PYNOD-tg2 mice were not significantly defective in IL-1β production upon *S. typhimurium* infection or R837 stimulation (data not shown). Thus, the suppressive effect of PYNOD in IL-1β production from 4 h PECs was confirmed in two independent transgenic mouse lines. In addition, these results suggest that neutrophils are more sensitive to PYNOD-overexpression than macrophages for their production of IL-1β.

Mouse PYNOD inhibits IL-1β production but not caspase-1 processing

Next, to explore the mechanism of the inhibitory effect of mouse PYNOD on IL-1β production, we investigated the processing of procaspase-1 in the mouse peritoneal macrophages after *S. typhimurium*

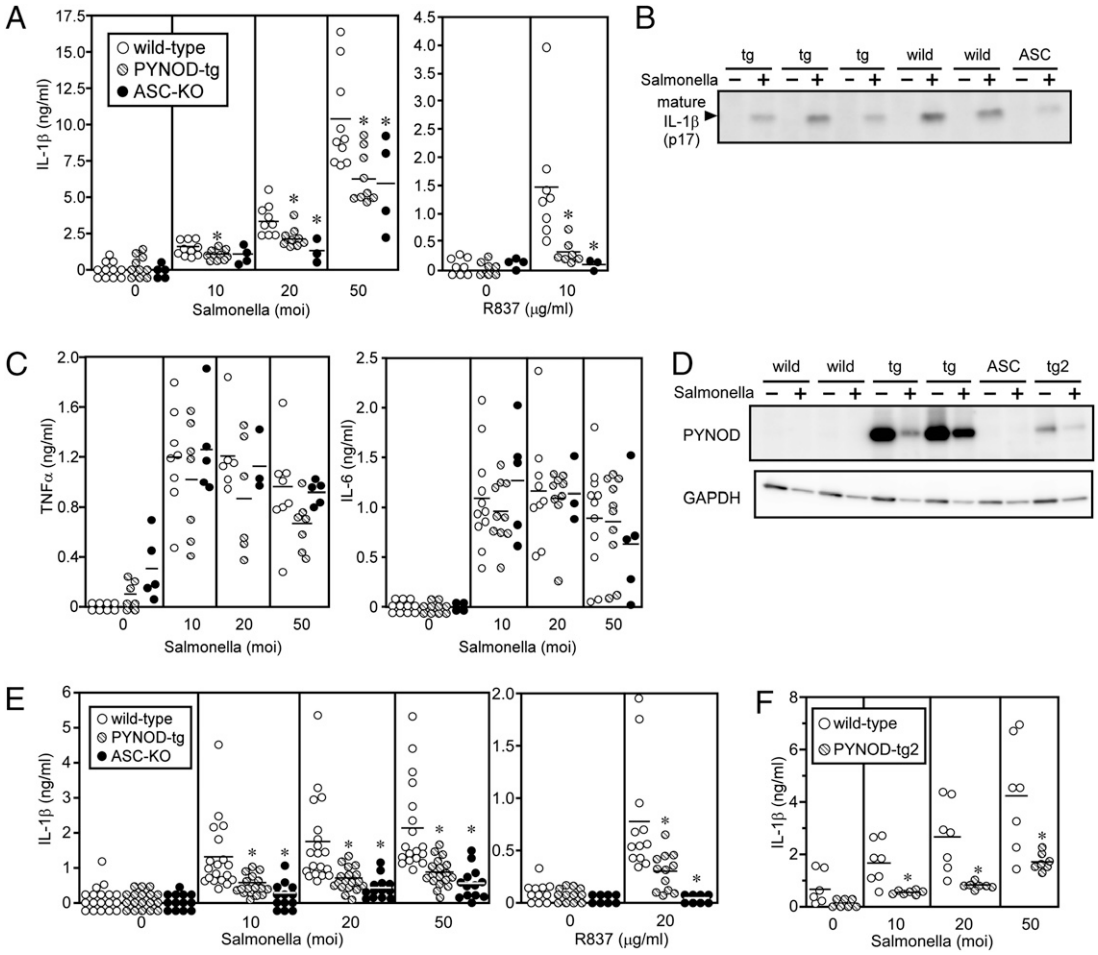

FIGURE 5. Peritoneal macrophages and neutrophil-rich 4-h PECs from PYNOD-tg mice exhibit reduced IL-1β secretion. *A–C*, Thioglycollate-induced macrophages from individual wild-type, PYNOD-tg, or ASC$^{-/-}$ mice were treated with (*A*, *B*) or without (*C*) LPS (1 μg/ml) for 16 h and then infected with *S. typhimurium* (moi 0, 10, 20, and 50) or stimulated with R837 (10 μg/ml). Twelve hours later, the culture supernatants were examined for IL-1β (*A*) or TNF-α and IL-6 (*C*) by ELISA. Each circle represents an individual mouse. Horizontal lines indicate the mean cytokine levels. The amount of mature IL-1β (p17) in the culture supernatant from wild-type, PYNOD-tg, or ASC$^{-/-}$ macrophages infected with *S. typhimurium* (moi 20) or left uninfected was assessed by immunoprecipitation followed by Western blot (*B*). *D–F*, Neutrophil-rich 4-h PECs from individual wild-type, PYNOD-tg, PYNOD-tg2, or ASC$^{-/-}$ mice were treated with LPS (1 μg/ml) for 16 h, then infected with *S. typhimurium* or stimulated with R837. In *D*, the amount of PYNOD in the lysate of cells infected with *S. typhimurium* at moi 20 or left uninfected for 2 h was examined by Western blot. Western blot for GAPDH serves as a loading control. In *E* and *F*, the amount of IL-1β in the culture supernatant after 12 h of infection or stimulation was determined by ELISA. Each circle represents one mouse. Horizontal lines indicate the mean cytokine level. Asterisks in *A*, *C*, *E*, and *F* indicate a statistically significant difference ($p < 0.05$) in the cytokine level compared with that of the wild-type control.

infection. Although the PYNOD-tg and ASC$^{-/-}$ macrophages produced reduced levels of IL-1β in response to *S. typhimurium* infection compared with those of wild-type macrophages (Fig. 5*A*), only the ASC$^{-/-}$ macrophages and not the PYNOD-tg macrophages showed a defect in procaspase-1 processing (Fig. 6*A*, *left panels*). The expression levels of pro–IL-1β, procaspase-1, and ASC in LPS-primed macrophages from wild-type and PYNOD-tg mice were similar to each other (Fig. 6*A*, *right panels*). Consistent with the ELISA data, PYNOD-tg macrophages produced reduced levels of mature IL-1β (p17) in response to *S. typhimurium* infection compared with those of wild-type macrophages, suggesting that the enzymatic activity of caspase-1 in PYNOD-tg macrophages was decreased without inhibiting procaspase-1 processing.

To clarify the reason why PYNOD inhibited IL-1β processing without inhibiting caspase-1 processing, we examined the mechanism of caspase-1 processing in peritoneal macrophages infected with *S. typhimurium* using caspase inhibitors with different specificities. As expected, IL-1β secretion was inhibited by both pan-caspase inhibitor z-VAD-fmk and caspase-1 inhibitor Ac-YVAD-cmk (Fig. 6*B*). In contrast, caspase-1 processing was inhibited by z-VAD-fmk but not by Ac-YVAD-cmk, suggesting that caspase-1 was processed by a certain caspase other than caspase-1 under these conditions. Because it was previously reported that casapse-11, a mouse homologue of caspase-4, is required for caspase-1 processing (31), we examined the effect of caspase-4 inhibitor z-LEED-fmk on caspase-1 processing. Interestingly, z-LEED-fmk inhibited caspase-1 processing in *S. typhimurium*-infected macrophages. Together with the previous report, these results suggest that PYNOD inhibited caspase-1–mediated IL-1β processing but not caspase-11–mediated caspase-1 processing.

ASC aggregation in PYNOD-tg macrophages is not suppressed

We also investigated the aggregation of ASC induced by R837 stimulation in LPS-primed peritoneal macrophages. As shown in Fig. 6*C*, the ASC aggregates in PYNOD-tg macrophages were comparable to those in wild-type macrophages. To compare the number and the size of ASC aggregates in wild-type and PYNOD-tg macrophages in the same microscopic fields, one of these two

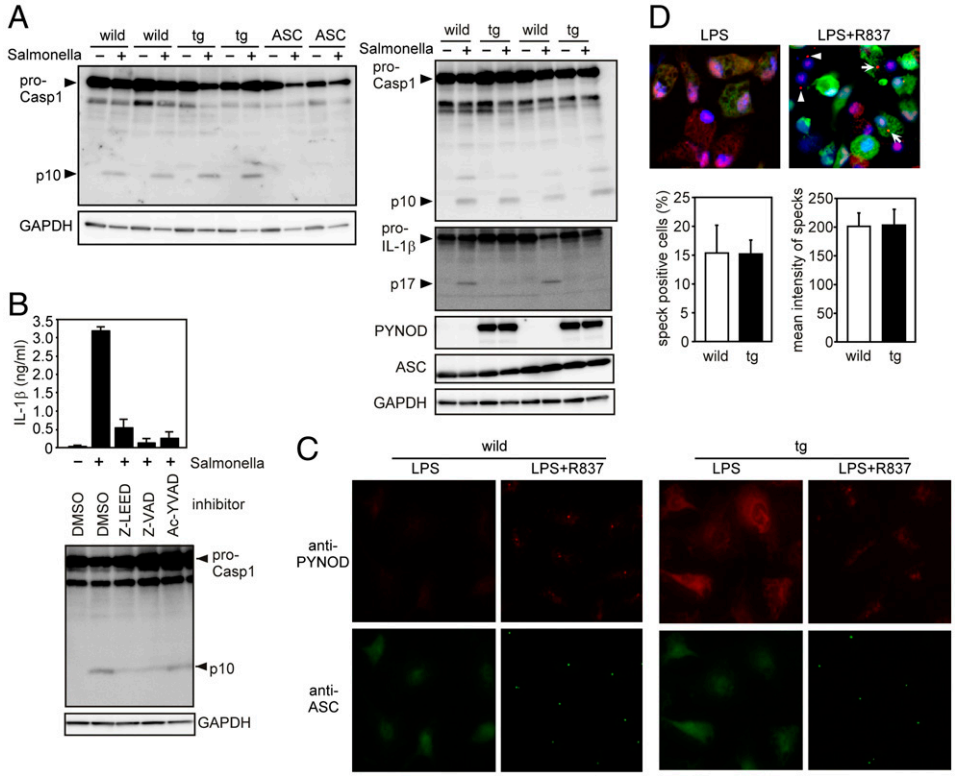

FIGURE 6. Neither caspase-1 processing nor ASC aggregation is inhibited in macrophages from PYNOD-tg mice. *A*, Thioglycollate-induced macrophages from individual wild-type, PYNOD-tg, or ASC$^{-/-}$ mice were pretreated with LPS as described in Fig. 3*E* and then infected with *S. typhimurium* (moi 50) or left uninfected for 2 h (*left*) or 10 min (*right*). The processing of caspase-1, IL-1β, and the expression of PYNOD and ASC were monitored by Western blot. Western blot for GAPDH serves as a loading control. *B*, Thioglycollate-induced macrophages from wild-type mouse were pretreated with LPS as described in *A*. The LPS-primed macrophages were then pretreated with the indicated inhibitors (20 μM) or DMSO (0.1%) for 1 h and further infected with *S. typhimurium* (moi 50) or left uninfected for 10 min. The amount of IL-1β in the culture supernatant postinfection was determined by ELISA. Experiments were done in duplicate, and error bars represent the range of duplicate samples. The processing of caspase-1 was monitored by Western blot. Western blot for GAPDH serves as a loading control. Data are representative of at least three independent experiments. z-LEED-fmk, caspase-4 inhibitor; z-VAD-fmk, pan-caspase inhibitor; Ac-YVAD-cmk, caspase-1 inhibitor. *C*, Thioglycollate-induced macrophages from wild-type or PYNOD-tg mice were pretreated with LPS as described in *A*. The LPS-primed macrophages were then cultured with or without R837 (50 μg/ml) for 1 h. The cells were stained for PYNOD (red) and ASC (green), as described in Fig. 3*E*. Original magnification ×250. *D*, Equal numbers of CFSE-labeled wild-type macrophages (green) and nonlabeled PYNOD-tg macrophages were cocultured on glass coverslips. Cells were primed with LPS and then stimulated with R837 or left unstimulated as described in *C*. The cells were stained with anti-ASC mAb followed by Cy3-conjugated anti-rat IgG (red) and DAPI (blue) and examined by confocal microscopy (*upper panels*). Arrows and arrowheads in the *upper right panel* indicate ASC aggregates in wild-type and PYNOD-tg macrophages, respectively. Original magnification ×220. Experiments were also done using nonlabeled wild-type and CFSE-labeled PYNOD-tg macrophages. The mean proportion of ASC aggregate-positive cells (*lower left panel*) and the mean fluorescence intensity of ASC aggregates (*lower right panel*) in LPS + R837-treated macrophages from wild-type and PYNOD-tg mice were calculated based on the data set obtained from the pair of experiments with reciprocal CFSE labeling. Error bars represent the range of the pairs of data.

macrophage populations was stained with CFSE and cocultured with the other one in the presence of LPS followed by R837 stimulation. ASC was then stained with anti-ASC mAb followed by a Cy3-labeled second Ab. Both mean intensity of ASC aggregates and percentage of ASC aggregate-positive cells were not suppressed in PYNOD-tg macrophages (Fig. 6*D*). Thus, unlike human PYNOD overexpressed with ASC in HEK293 cells, mouse PYNOD did not inhibit ASC aggregation in macrophages.

PYNOD-tg mice are resistant to LPS-induced endotoxic shock

A high dose of LPS leads to endotoxic shock and death in mice, presumably due to the massive, systemic release of proinflammatory cytokines. Caspase-1 and ASC are important mediators of this inflammatory response (27, 30, 32). To examine the role of PYNOD in this response, we injected lethal doses (30 and 50 mg/kg) of LPS into wild-type, PYNOD-tg, and ASC$^{-/-}$ mice (Fig. 7*A*). Consistent with previous reports (30), the ASC$^{-/-}$ mice showed enhanced survival following the LPS injection. Notably, the survival of the PYNOD-tg mice was also significantly enhanced. Unlike cytokine production from PYNOD-tg macrophages, serum levels of not only IL-1β but also TNF-α after LPS injection were decreased in PYNOD-tg and ASC$^{-/-}$ mice compared with those of wild-type mice (Fig. 7*B*). These results indicate that PYNOD influence not only IL-1β but also TNF-α production in vivo and that PYNOD is a potential negative regulator of LPS-induced endotoxic shock.

Discussion

In this study, we first investigated the molecular basis of human PYNOD's inhibition of caspase-1–mediated IL-1β secretion and of ASC-mediated NF-κB activation and apoptosis. We found that human PYNOD inhibited the autoprocessing of procaspase-1 through its NOD but not its PYD. Because the NOD of PYNOD, but not its PYD, interacted with caspase-1, it is likely that the PYNOD's NOD inhibited the catalytic activity of caspase-1 or the self-oligomerization of caspase-1, which would be required for the autoprocessing of caspase-1. We could not detect the expression of NLRP3 and NLRC4 proteins in HEK293T cells (data not shown). However, we cannot exclude an alternative possibility that the

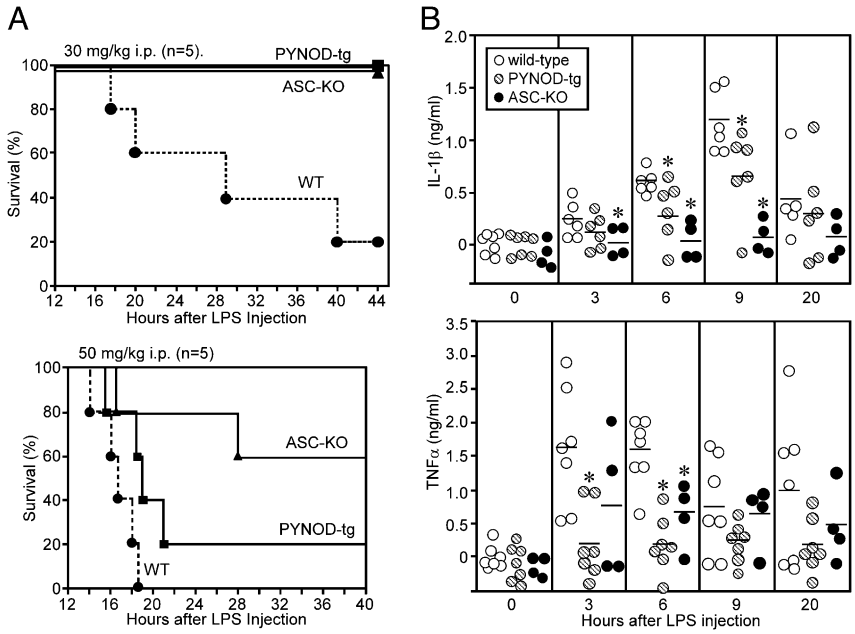

FIGURE 7. PYNOD-tg mice are resistant to LPS-induced endotoxic shock. *A*, Wild-type, PYNOD-tg, and ASC$^{-/-}$ mice (8- to 10-wk-old) were i.p. injected with 30 or 50 mg/kg LPS (*E. coli* 0111:B4) as indicated, and their survival was monitored. *B*, Serum levels of IL-1β and TNF-α after i.p. injection of 30 mg/kg LPS were measured by ELISA. Each circle represents one mouse. Horizontal lines indicate the mean cytokine level. Asterisks indicate statistically significant difference ($p < 0.05$) in the cytokine production compared with that in the wild-type mice.

PYNOD's NOD inhibited the oligomerization of a certain endogenous NLR protein that might contribute to the caspase-1 autoprocessing through a heterogeneous NOD–NOD interaction. In contrast, the PYD of human PYNOD inhibited ASC-mediated NF-κB activation and apoptosis and ASC's ability to promote caspase-1–mediated IL-1β production. Because pyrin, which gives its name to PYD, is a physiological inhibitor of ASC (33), the PYD of pyrin and ASC may have a common function. Thus, human PYNOD seems to exert its anti-inflammatory activity by inhibiting the activation of caspase-1 and ASC using distinct domains, NOD and PYD, respectively. These domains could achieve each function independently (Figs. 1*C*, 1*E*, 2*A*, 2*B*). However, cooperation of these two functional domains may be important for effective inhibition of ASC's functions to induce inflammation and cell death under physiological conditions. We also found that human PYNOD inhibited the formation of ASC aggregates in this study. Although the physiological role of ASC aggregates is still unclear, it was previously reported that caspase-1 was copurified with ASC aggregates from THP-1 cells (34). In addition, we previously reported that caspase-8 is colocalized with ASC and is important for ASC-mediated NF-κB activation and apoptosis (9, 10). Therefore, ASC aggregates may play a role as a platform for caspase-1 activation, caspase-8 activation, or both, and human PYNOD might block the activation of caspases by inhibiting ASC aggregation.

We previously reported that human PYNOD mRNA is ubiquitously expressed in various tissues, with the highest expression in the brain, heart, and skeletal muscle. In the current study, we found that mouse PYNOD protein had a more restricted expression pattern, appearing only in the skin, tongue, and heart. This expression pattern agrees well with mouse PYNOD's mRNA expression profile, extracted from a comprehensive gene expression data set for mouse tissues (Mouse GNF1M, gcRMA, available at http://symatlas.gnf.org/SymAtlas/, the Web site of the Genomics Institute of the Novartis Research Foundation). Although we do not know the function of PYNOD in these tissues, they also express mRNAs for ASC, caspase-1, and/or IL-18 at high levels, so it is possible that PYNOD regulates the function of these proteins in these organs. Although we failed to detect PYNOD protein in mouse skeletal muscle, we found that the C_2C_{12} myoblastoma line expresses PYNOD. Therefore, mouse myocytes may express PYNOD under certain conditions.

Consistent with the notion that PYNOD is a negative regulator of inflammatory responses, we found that mouse PYNOD protein was expressed in thioglycollate-induced peritoneal macrophages as well as in macrophagic and dendritic cell lines. We also demonstrated in this study for the first time that the transgenic expression of mouse PYNOD in macrophages inhibits the IL-1β production induced by microbial infection, consistent with our previous finding that human PYNOD inhibits caspase-1–mediated IL-1β secretion. Furthermore, the PYNOD-tg mice were resistant to LPS-induced endotoxic shock. These results strongly support our hypothesis that PYNOD functions as negative regulator of inflammation in vivo by inhibiting IL-1β secretion, although further proof will require the development of PYNOD-deficient mice.

We also found that speck-like aggregates of ASC were formed under inflammatory conditions that induced caspase-1–mediated IL-1β secretion in macrophages. In contrast, Fas ligand, which induces the caspase-1–independent secretion of mature IL-1β (25), did not induce ASC speck formation. Therefore, the appearance of ASC specks in macrophages correlated well with caspase-1–mediated IL-1β secretion. Interestingly, PYNOD colocalized with ASC aggregates in R837-stimulated macrophages. However, in contrast to human PYNOD, mouse PYNOD did not inhibit ASC aggregation in the peritoneal macrophages from PYNOD-tg mice. Although we have not yet clarified the significance of mouse PYNOD's colocalization with ASC aggregates, because caspase-1 also colocalizes with ASC aggregates (34 and data not shown), mouse PYNOD might inhibit recruitment of caspase-1 to ASC, the catalytic activity of caspase-1 in ASC aggregates, or both. Alternatively, because we previously found that PYNOD interacts with pro–IL-1β (11), PYNOD might inhibit IL-1β processing by interacting with this substrate.

It has been demonstrated that ASC is dispensable for NF-κB–dependent cytokine expression in mouse macrophages (27, 30). Consistent with this observation, the PYNOD-tg macrophages exhibited a normal capacity to produce TNF-α and IL-6 upon *S. typhimurium* infection. However, the expression of exogenous human ASC induces NF-κB activation in HEK293 cells, and PYNOD inhibits this response. In addition, the knockdown of ASC expression in human macrophagic cell lines results in the suppression of NF-κB activation and cytokine production in response to microbial stimuli (35). Thus, it is likely that ASC plays an important

role in the activation of NF-κB upon microbial infection in humans, and our finding that PYNOD did not inhibit TNF-α and IL-6 production in mouse macrophages may not extend to humans. Furthermore, decreased levels of TNF-α were detected in sera from PYNOD-tg, and $ASC^{-/-}$ mice after LPS injection. Therefore, it is possible that ASC plays a crucial role in LPS-induced TNF-α production in certain mouse cells other than macrophages, and PYNOD may have a capacity to inhibit this response.

Nod1, Nod2, NLRC4, NLRP1, and NLRP3 play important roles in the recognition of pathogens and the initiation of innate immune responses, as described above. In addition, NLRP6 (also called PYPAF5, NALP6, CLR11.4, and PAN3) and NLRP12 can induce NF-κB activation and caspase-1–mediated IL-1β maturation (7, 36), whereas CIITA (NLRA) is essential for the expression of class II MHC (37). Thus, these proteins constitute a proinflammatory subfamily of the NLRs. In contrast, we previously showed that human PYNOD inhibits ASC and the activation of caspase-1 and thus is a potential anti-inflammatory factor (11). Consistent with this idea, in this study, we demonstrated that macrophages derived from PYNOD-tg mice produced reduced levels of IL-1β in response to inflammatory stimulation. Interestingly, we also found that NLRP7 inhibits caspase-1–dependent IL-1β processing, whereas NLRP2 inhibits ASC-mediated NF-κB activation (12). NLRP4 was reported to inhibit the NF-κB activation induced by TNF-α or IL-1β (13), whereas NLRC3 is highly expressed in T cells and inhibits anti-CD3 and CD28-induced NF-κB, NFAT, and AP-1 activation and thereby IL-2 and CD25 expression in Jurkat cells (14). In conflict with above-described proinflammatory function of NLRP12, it was recently reported that NLRP12 inhibits noncanonical NF-κB activation (17). In addition, Nod2-S, a short isoform of Nod2 that is preferentially expressed in the human colon, interacts with Nod2 and RIP2/RICK to inhibit the proinflammatory signals of Nod2 (16). Recently, NLRX1 was reported to localize to the mitochondrial outer membrane and inhibit mitochondrial antiviral signaling-mediated activation of the IFN-β promoter and NF-κB (15). Although evidence for antiapoptotic functions of these NLRs is still preliminary, given the detrimental nature of inflammation, it is reasonable to expect that anti-inflammatory NLRs should exist. Therefore, we propose that these NLRs constitute an anti-inflammatory subgroup. Further study of these anti-inflammatory NLRs will increase our understanding of the innate immune system.

It should also be noted that certain proinflammatory NLR members are associated with inflammatory disease. For example, allelic variants of the *Nod2* gene are associated with Crohn's disease, Blau syndrome, and early-onset sarcoidosis (38–41), whereas those of NLRP3 or NLRP12 cause periodical fever syndromes (42–44). Importantly, mutations in *MEFV*, the gene encoding pyrin, also cause familial Mediterranean fever, a type of periodical fever syndrome (45, 46). Because PYNOD seems to have a function similar to that of pyrin, a defect in PYNOD might cause similar diseases.

Although further analyses of the in vivo function of PYNOD await the generation of a PYNOD-deficient mouse, our findings suggest that PYNOD is the first NLR family member to show an inhibitory effect on inflammation in vivo.

Acknowledgments

We thank Dr. G. Yamada (Kumamoto University) for providing the plasmid pCAGGS and helping to establish PYNOD-tg mice. We also thank H. Kushiyama for secretarial and technical assistance.

Disclosures

The authors have no financial conflicts of interest.

References

1. Tschopp, J., F. Martinon, and K. Burns. 2003. NALPs: a novel protein family involved in inflammation. *Nat. Rev. Mol. Cell Biol.* 4: 95–104.
2. Inohara, N., and G. Nuñez. 2003. NODs: intracellular proteins involved in inflammation and apoptosis. *Nat. Rev. Immunol.* 3: 371–382.
3. Inohara, N., T. Koseki, L. del Peso, Y. Hu, C. Yee, S. Chen, R. Carrio, J. Merino, D. Liu, J. Ni, and G. Núñez. 1999. Nod1, an Apaf-1-like activator of caspase-9 and nuclear factor-kappaB. *J. Biol. Chem.* 274: 14560–14567.
4. Martinon, F., V. Pétrilli, A. Mayor, A. Tardivel, and J. Tschopp. 2006. Gout-associated uric acid crystals activate the NALP3 inflammasome. *Nature* 440: 237–241.
5. Dostert, C., V. Pétrilli, R. Van Bruggen, C. Steele, B. T. Mossman, and J. Tschopp. 2008. Innate immune activation through Nalp3 inflammasome sensing of asbestos and silica. *Science* 320: 674–677.
6. Srinivasula, S. M., J. L. Poyet, M. Razmara, P. Datta, Z. J. Zhang, and E. S. Alnemri. 2002. The PYRIN-CARD protein ASC is an activating adaptor for caspase-1. *J. Biol. Chem.* 277: 21119–21122.
7. Wang, L., G. A. Manji, J. M. Grenier, A. Al-Garawi, S. Merriam, J. M. Lora, B. J. Geddes, M. Briskin, P. S. DiStefano, and J. Bertin. 2002. PYPAF7, a novel PYRIN-containing Apaf1-like protein that regulates activation of NF-kappa B and caspase-1-dependent cytokine processing. *J. Biol. Chem.* 277: 29874–29880.
8. Martinon, F., and J. Tschopp. 2007. Inflammatory caspases and inflammasomes: master switches of inflammation. *Cell Death Differ.* 14: 10–22.
9. Hasegawa, M., R. Imamura, T. Kinoshita, N. Matsumoto, J. Masumoto, N. Inohara, and T. Suda. 2005. ASC-mediated NF-kappaB activation leading to interleukin-8 production requires caspase-8 and is inhibited by CLARP. *J. Biol. Chem.* 280: 15122–15130.
10. Hasegawa, M., K. Kawase, N. Inohara, R. Imamura, W. C. Yeh, T. Kinoshita, and T. Suda. 2007. Mechanism of ASC-mediated apoptosis: bid-dependent apoptosis in type II cells. *Oncogene* 26: 1748–1756.
11. Wang, Y., M. Hasegawa, R. Imamura, T. Kinoshita, C. Kondo, K. Konaka, and T. Suda. 2004. PYNOD, a novel Apaf-1/CED4-like protein is an inhibitor of ASC and caspase-1. *Int. Immunol.* 16: 777–786.
12. Kinoshita, T., Y. Wang, M. Hasegawa, R. Imamura, and T. Suda. 2005. PYPAF3, a PYRIN-containing APAF-1-like protein, is a feedback regulator of caspase-1-dependent interleukin-1beta secretion. *J. Biol. Chem.* 280: 21720–21725.
13. Fiorentino, L., C. Stehlik, V. Oliveira, M. E. Ariza, A. Godzik, and J. C. Reed. 2002. A novel PAAD-containing protein that modulates NF-kappa B induction by cytokines tumor necrosis factor-alpha and interleukin-1beta. *J. Biol. Chem.* 277: 35333–35340.
14. Conti, B. J., B. K. Davis, J. Zhang, W. O'Connor, Jr., K. L. Williams, and J. P. Ting. 2005. CATERPILLER 16.2 (CLR16.2), a novel NBD/LRR family member that negatively regulates T cell function. *J. Biol. Chem.* 280: 18375–18385.
15. Moore, C. B., D. T. Bergstralh, J. A. Duncan, Y. Lei, T. E. Morrison, A. G. Zimmermann, M. A. Accavitti-Loper, V. J. Madden, L. Sun, Z. Ye, et al. 2008. NLRX1 is a regulator of mitochondrial antiviral immunity. *Nature* 451: 573–577.
16. Rosenstiel, P., K. Huse, A. Till, J. Hampe, S. Hellmig, C. Sina, S. Billmann, O. von Kampen, G. H. Waetzig, M. Platzer, et al. 2006. A short isoform of NOD2/CARD15, NOD2-S, is an endogenous inhibitor of NOD2/receptor-interacting protein kinase 2-induced signaling pathways. *Proc. Natl. Acad. Sci. USA* 103: 3280–3285.
17. Lich, J. D., K. L. Williams, C. B. Moore, J. C. Arthur, B. K. Davis, D. J. Taxman, and J. P. Ting. 2007. Monarch-1 suppresses non-canonical NF-kappaB activation and p52-dependent chemokine expression in monocytes. *J. Immunol.* 178: 1256–1260.
18. Imamura, R., K. Konaka, N. Matsumoto, M. Hasegawa, M. Fukui, N. Mukaida, T. Kinoshita, and T. Suda. 2004. Fas ligand induces cell-autonomous NF-kappaB activation and interleukin-8 production by a mechanism distinct from that of tumor necrosis factor-alpha. *J. Biol. Chem.* 279: 46415–46423.
19. Kanegae, Y., G. Lee, Y. Sato, M. Tanaka, M. Nakai, T. Sakaki, S. Sugano, and I. Saito. 1995. Efficient gene activation in mammalian cells by using recombinant adenovirus expressing site-specific Cre recombinase. *Nucleic Acids Res.* 23: 3816–3821.
20. Miyazaki, J., S. Takaki, K. Araki, F. Tashiro, A. Tominaga, K. Takatsu, and K. Yamamura. 1989. Expression vector system based on the chicken beta-actin promoter directs efficient production of interleukin-5. *Gene* 79: 269–277.
21. Niwa, H., K. Yamamura, and J. Miyazaki. 1991. Efficient selection for high-expression transfectants with a novel eukaryotic vector. *Gene* 108: 193–199.
22. Miwa, K., H. Hashimoto, T. Yatomi, N. Nakamura, S. Nagata, and T. Suda. 1999. Therapeutic effect of an anti-Fas ligand mAb on lethal graft-versus-host disease. *Int. Immunol.* 11: 925–931.
23. Miyamoto, A., T. Kunisada, H. Hemmi, T. Yamane, H. Yasuda, K. Miyake, H. Yamazaki, and S. I. Hayashi. 1998. Establishment and characterization of an immortal macrophage-like cell line inducible to differentiate to osteoclasts. *Biochem. Biophys. Res. Commun.* 242: 703–709.
24. Rock, K. L., L. Rothstein, S. Gamble, and C. Fleischacker. 1993. Characterization of antigen-presenting cells that present exogenous antigens in association with class I MHC molecules. *J. Immunol.* 150: 438–446.
25. Miwa, K., M. Asano, R. Horai, Y. Iwakura, S. Nagata, and T. Suda. 1998. Caspase 1-independent IL-1beta release and inflammation induced by the apoptosis inducer Fas ligand. *Nat. Med.* 4: 1287–1292.
26. Myint, K. M., Y. Yamamoto, T. Doi, I. Kato, A. Harashima, H. Yonekura, T. Watanabe, H. Shinohara, M. Takeuchi, K. Tsuneyama, et al. 2006. RAGE control of diabetic nephropathy in a mouse model: effects of RAGE gene

disruption and administration of low-molecular weight heparin. *Diabetes* 55: 2510–2522.
27. Yamamoto, M., K. Yaginuma, H. Tsutsui, J. Sagara, X. Guan, E. Seki, K. Yasuda, M. Yamamoto, S. Akira, K. Nakanishi, et al. 2004. ASC is essential for LPS-induced activation of procaspase-1 independently of TLR-associated signal adaptor molecules. *Genes Cells* 9: 1055–1067.
28. Masumoto, J., S. Taniguchi, K. Ayukawa, H. Sarvotham, T. Kishino, N. Niikawa, E. Hidaka, T. Katsuyama, T. Higuchi, and J. Sagara. 1999. ASC, a novel 22-kDa protein, aggregates during apoptosis of human promyelocytic leukemia HL-60 cells. *J. Biol. Chem.* 274: 33835–33838.
29. Kanneganti, T. D., N. Ozören, M. Body-Malapel, A. Amer, J. H. Park, L. Franchi, J. Whitfield, W. Barchet, M. Colonna, P. Vandenabeele, et al. 2006. Bacterial RNA and small antiviral compounds activate caspase-1 through cryopyrin/Nalp3. *Nature* 440: 233–236.
30. Mariathasan, S., K. Newton, D. M. Monack, D. Vucic, D. M. French, W. P. Lee, M. Roose-Girma, S. Erickson, and V. M. Dixit. 2004. Differential activation of the inflammasome by caspase-1 adaptors ASC and Ipaf. *Nature* 430: 213–218.
31. Wang, S., M. Miura, Y. K. Jung, H. Zhu, E. Li, and J. Yuan. 1998. Murine caspase-11, an ICE-interacting protease, is essential for the activation of ICE. *Cell* 92: 501–509.
32. Li, P., H. Allen, S. Banerjee, S. Franklin, L. Herzog, C. Johnston, J. McDowell, M. Paskind, L. Rodman, J. Salfeld, et al. 1995. Mice deficient in IL-1 beta-converting enzyme are defective in production of mature IL-1 beta and resistant to endotoxic shock. *Cell* 80: 401–411.
33. Dowds, T. A., J. Masumoto, F. F. Chen, Y. Ogura, N. Inohara, and G. Núñez. 2003. Regulation of cryopyrin/Pypaf1 signaling by pyrin, the familial Mediterranean fever gene product. *Biochem. Biophys. Res. Commun.* 302: 575–580.
34. Fernandes-Alnemri, T., J. Wu, J.-W. Yu, P. Datta, B. Miller, W. Jankowski, S. Rosenberg, J. Zhang, and E. S. Alnemri. 2007. The pyroptosome: a supramolecular assembly of ASC dimers mediating inflammatory cell death via caspase-1 activation. *Cell Death Differ.* 14: 1590–1604.
35. Taxman, D. J., J. Zhang, C. Champagne, D. T. Bergstralh, H. A. Iocca, J. D. Lich, and J. P. Y. Ting. 2006. Cutting edge: ASC mediates the induction of multiple cytokines by *Porphyromonas gingivalis* via caspase-1-dependent and -independent pathways. *J. Immunol.* 177: 4252–4256.
36. Grenier, J. M., L. Wang, G. A. Manji, W. J. Huang, A. Al-Garawi, R. Kelly, A. Carlson, S. Merriam, J. M. Lora, M. Briskin, et al. 2002. Functional screening of five PYPAF family members identifies PYPAF5 as a novel regulator of NF-kappaB and caspase-1. *FEBS Lett.* 530: 73–78.
37. Steimle, V., L. A. Otten, M. Zufferey, and B. Mach. 1993. Complementation cloning of an MHC class II transactivator mutated in hereditary MHC class II deficiency (or bare lymphocyte syndrome). *Cell* 75: 135–146.
38. Ogura, Y., D. K. Bonen, N. Inohara, D. L. Nicolae, F. F. Chen, R. Ramos, H. Britton, T. Moran, R. Karaliuskas, R. H. Duerr, et al. 2001. A frameshift mutation in NOD2 associated with susceptibility to Crohn's disease. *Nature* 411: 603–606.
39. Miceli-Richard, C., S. Lesage, M. Rybojad, A. M. Prieur, S. Manouvrier-Hanu, R. Häfner, M. Chamaillard, H. Zouali, G. Thomas, and J. P. Hugot. 2001. CARD15 mutations in Blau syndrome. *Nat. Genet.* 29: 19–20.
40. Hugot, J. P., M. Chamaillard, H. Zouali, S. Lesage, J. P. Cézard, J. Belaiche, S. Almer, C. Tysk, C. A. O'Morain, M. Gassull, et al. 2001. Association of NOD2 leucine-rich repeat variants with susceptibility to Crohn's disease. *Nature* 411: 599–603.
41. Kanazawa, N., I. Okafuji, N. Kambe, R. Nishikomori, M. Nakata-Hizume, S. Nagai, A. Fuji, T. Yuasa, A. Manki, Y. Sakurai, et al. 2005. Early-onset sarcoidosis and CARD15 mutations with constitutive nuclear factor-kappaB activation: common genetic etiology with Blau syndrome. *Blood* 105: 1195–1197.
42. Hoffman, H. M., J. L. Mueller, D. H. Broide, A. A. Wanderer, and R. D. Kolodner. 2001. Mutation of a new gene encoding a putative pyrin-like protein causes familial cold autoinflammatory syndrome and Muckle-Wells syndrome. *Nat. Genet.* 29: 301–305.
43. Feldmann, J., A. M. Prieur, P. Quartier, P. Berquin, S. Certain, E. Cortis, D. Teillac-Hamel, A. Fischer, and G. de Saint Basile. 2002. Chronic infantile neurological cutaneous and articular syndrome is caused by mutations in CIAS1, a gene highly expressed in polymorphonuclear cells and chondrocytes. *Am. J. Hum. Genet.* 71: 198–203.
44. Jéru, I., P. Duquesnoy, T. Fernandes-Alnemri, E. Cochet, J. W. Yu, M. Lackmy-Port-Lis, E. Grimprel, J. Landman-Parker, V. Hentgen, S. Marlin, et al. 2008. Mutations in NALP12 cause hereditary periodic fever syndromes. *Proc. Natl. Acad. Sci. USA* 105: 1614–1619.
45. French FMF Consortium. 1997. A candidate gene for familial Mediterranean fever. *Nat. Genet.* 17: 25–31.
46. The International FMF Consortium. 1997. Ancient missense mutations in a new member of the RoRet gene family are likely to cause familial Mediterranean fever. *Cell* 90: 797–807.